

Study Regarding the Influence of the Plate Heat Exchanger Configuration on Its Performance

ROXANA GRIGORE, SORIN POPA, ANETA HAZI, GHEORGHE HAZI

Power Engineering Department
 “Vasile Alecsandri” University of Bacau
 Bacau, Calea Marasesti no.157
 ROMANIA
 rgrigore@ub.ro

Abstract: The paper presents an analysis related to the correlation between the performance of plate heat exchanger and its number of plates. There are taken into consideration eight different cases obtained by changing the plate's number of a heat exchanger and using finite element method numerical simulations of fluid flow distribution. Numerical results are presented for 1 pass -1pass counter-flow plate heat exchanger. These results are shown in terms of cold water temperature at the outlet, hot water temperature at the outlet, exchanger effectiveness and log – mean temperature difference as functions of the heat capacity ratio and the number of plates.

Key-Words: - plate heat exchanger, finite element method, mesh, fluid flow, number of plates, heat exchanger effectiveness, log mean temperature difference

1 Introduction

Plate heat exchangers are very common equipments used in industrial applications. These are used to exchange heat between two fluids, cooling and heating processes, heat recovery. Plate heat exchangers have a lot of advantages, including a high heat exchange area per unit volume and good heat transfer performance [1].

An important number of numerical studies applying finite element method has been made to research fluid flow and heat transfer into plate heat exchangers [2], [3], [4],[5]. It was studied the optimal configuration of a heat exchanger, too [6], [7].

The paper presents some aspects about the influence of number of plates on heat transfer in a plate heat exchanger. Eight constructive cases are considered, obtained by changing the number of thermal plates. Meanwhile, the paper represents a continuation of research in [8], [9] and tackle them from a new perspective.

Geometric models are realized using SolidWorks. To realize the proposed studies, applications based on computer simulation of fluid flow are made using COSMOS/Flow.

2 Presentation of studied plate heat exchangers

The studied heat exchangers are a pack of few stainless steel flat plates with gaskets. The hot water flows are in one direction in alternating chambers while the cold water flows are in counter flow in the other alternating

chambers. The number of passes is 1 and the thermal agents are directed into their proper chambers either by a suitable gasket made from rubber EPDM [8]. The width of channel between plates is 0,004 m. The geometric dimensions of the thermal plate are represented in table 1.

Dimension	Notation	Value	Unit
Diameter of the inlet tube	d	0,002	m
Effective plate length	L	0,43	m
Effective plate width	l	0,13	m
Stainless steel plate thickness	δ_p	0,002	m

Table 1. Geometric dimensions of the plate

Heat exchangers are used to warm the cold water, considered a secondary thermal agent, with hot water, a primary thermal agent. We are interested to get as high the outlet cold water temperature with higher heat exchanger effectiveness as well.

The influence of the number of plates on heat transfer is investigated considering a variable number of plates: 3,4,5,6,7,8,9,10 plates. It is important to note that the heat exchangers are 1pass-1pass counter-flow plate heat exchangers. Figure 1 shows the functional scheme of a heat exchanger with 4 plates –an even number of plates and the functional scheme for the case with odd number of plates, 5 plates respectively. It is

observed that for a counter-flow plate heat exchanger with an odd number of plates, the number of flow channels is identical for hot and cold water. For a counter-flow exchanger with an even number of plates, in the studied cases, the number of flow channels for hot water is one greater than for cold water.

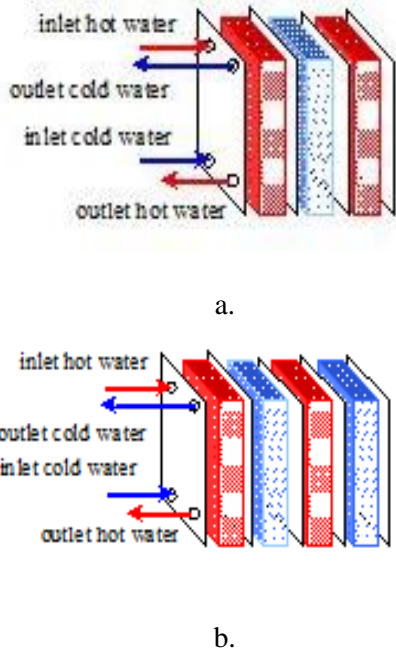


Fig.1. The functional scheme of plate heat exchanger
a.4 plates, b.5 plates

3D geometric models of the heat exchangers are created using SolidWorks program. Figure 2 shows the model of plate heat exchanger with 10 plates and in figure 3 is shown the model of counter-flow heat exchanger with 3 plates.

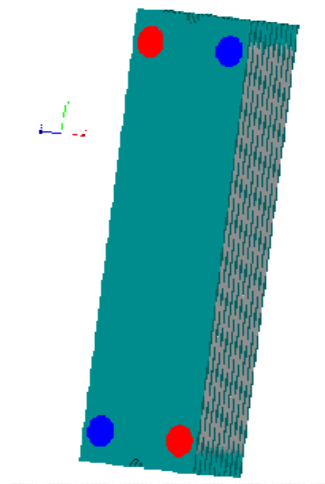


Fig.2. 3D model of counter-flow plate heat exchanger with 10 plates

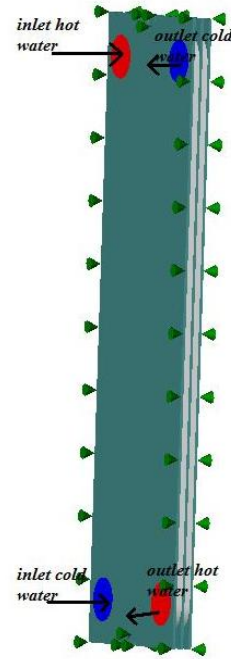


Fig.3. 3D model of counter-flow plate heat exchanger with 3 plates

3 Mathematical modeling of plate heat exchangers

Mathematical modeling is based on the governing equations which include the continuity equations, the Navier-Stokes equations and the energy equation. These equations are intimately coupled and non-linear making a general analytic solution almost impossible. The governing pdes can be written as [9], [10]:

Continuity equation:

$$\frac{\partial \rho}{\partial t} + \frac{\partial \rho u}{\partial x} + \frac{\partial \rho v}{\partial y} + \frac{\partial \rho w}{\partial z} = 0 \quad (1)$$

x-,y-,z-, momentum equations:

$$\begin{aligned} \rho \frac{\partial u}{\partial t} + \rho u \frac{\partial u}{\partial x} + \rho v \frac{\partial u}{\partial y} + \rho w \frac{\partial u}{\partial z} &= \\ &= \rho g_x - \frac{\partial p}{\partial x} + \frac{\partial}{\partial x} \left[2\eta \frac{\partial u}{\partial x} \right] + \frac{\partial}{\partial y} \left[\eta \left(\frac{\partial u}{\partial y} + \frac{\partial v}{\partial x} \right) \right] + \frac{\partial}{\partial z} \left[\eta \left(\frac{\partial u}{\partial z} + \frac{\partial w}{\partial x} \right) \right] + S_{\omega} + S_{DR} \\ \rho \frac{\partial v}{\partial t} + \rho u \frac{\partial v}{\partial x} + \rho v \frac{\partial v}{\partial y} + \rho w \frac{\partial v}{\partial z} &= \\ &= \rho g_y - \frac{\partial p}{\partial y} + \frac{\partial}{\partial y} \left[2\eta \frac{\partial v}{\partial y} \right] + \frac{\partial}{\partial x} \left[\eta \left(\frac{\partial u}{\partial y} + \frac{\partial v}{\partial x} \right) \right] + \frac{\partial}{\partial z} \left[\eta \left(\frac{\partial v}{\partial z} + \frac{\partial w}{\partial y} \right) \right] + S_{\omega} + S_{DR} \\ \rho \frac{\partial w}{\partial t} + \rho u \frac{\partial w}{\partial x} + \rho v \frac{\partial w}{\partial y} + \rho w \frac{\partial w}{\partial z} &= \\ &= \rho g_z - \frac{\partial p}{\partial z} + \frac{\partial}{\partial z} \left[2\eta \frac{\partial w}{\partial z} \right] + \frac{\partial}{\partial x} \left[\eta \left(\frac{\partial u}{\partial z} + \frac{\partial w}{\partial x} \right) \right] + \frac{\partial}{\partial y} \left[\eta \left(\frac{\partial v}{\partial z} + \frac{\partial w}{\partial y} \right) \right] + S_{\omega} + S_{DR} \end{aligned} \quad (2)$$

The two source terms in the momentum equations, S_ω and S_{DR} , are for rotating coordinates and distributed resistances, respectively. The distributed resistance term can be written in general as [8]:

$$S_{DR} = -\left(K_i + \frac{f}{d}\right) \frac{\rho V_i^2}{2} - C\eta V_i, \quad (3)$$

where i refer to the global coordinate direction (u, v, w momentum equation), f - friction factor, d - hydraulic diameter, C - permeability and the other factors are described in table 2. Note that the K -factor term can operate on a single momentum equation at a time because each direction has its own unique K -factor. The other two resistance types operate equally on each momentum equation [8], [10]. Distributed resistance can be used to reduce the overall size of the problem.

The other source term is for rotating flow. This term can be written in general as [8]:

$$S_\omega = -2\rho\omega_i \times V_i - \rho\omega_i \times \omega_i \times r_i, \quad (4)$$

where i refer to the global coordinate direction, ω - rotational speed and r - distance from the axis of rotation.

For incompressible and subsonic compressible flow, the energy equation is written in terms of static temperature [8]:

$$\begin{aligned} \rho c_p \frac{\partial T}{\partial t} + \rho c_p u \frac{\partial T}{\partial x} + \rho c_p v \frac{\partial T}{\partial y} + \rho c_p w \frac{\partial T}{\partial z} = \\ = \frac{\partial}{\partial x} \left[k \frac{\partial T}{\partial x} \right] + \frac{\partial}{\partial y} \left[k \frac{\partial T}{\partial y} \right] + \frac{\partial}{\partial z} \left[k \frac{\partial T}{\partial z} \right] + q_v \end{aligned} \quad (5)$$

The volumetric heat source term from equation (5) is considered zero for this model.

Table 2 presents the variable of the equations:

Variable	Description
c_p	specific heat at constant pressure
k	thermal conductivity
p	pressure
q_v	volumetric heat source
T	temperature
t	time
u	velocity component in x-direction
v	velocity component in y-direction
w	velocity component in z-direction
ρ	density
η	dynamic viscosity

Table 2. Variable of the governing equation

The equations describe the fluid flow and heat transfer under steady-state conditions for Cartesian geometries. For the turbulent flow, the solution of these equations would require a great deal of finite elements (on the order of $10^6 - 10^8$) even for a simple geometry as well as near infinitesimal time steps. COSMOS/Flow solves the *time-averaged* governing equations.

The time-averaged equations are obtained by assuming that the dependent variables can be represented as a superposition of a mean value and a fluctuating value, where the fluctuation is about the mean [8]. For example, the velocity component in y-direction can be written:

$$V = V + v', \text{ [m/s]} \quad (6)$$

where V [m/s] – the mean velocity, v' [m/s] – the fluctuation about the mean. This representation is introduced into the governing equations and the equations themselves are averaged over time.

If we use the notation that the uppercase letters represent the mean values and lowercase letters represent fluctuating values, it can be written the governing equations[10]:

continuity equation:

$$\frac{\partial \rho}{\partial t} + \frac{\partial \rho u}{\partial x} + \frac{\partial \rho v}{\partial y} + \frac{\partial \rho w}{\partial z} = 0, \quad (7)$$

momentum equations:

$$\begin{aligned} \rho \frac{\partial U}{\partial t} + \rho U \frac{\partial U}{\partial x} + \rho V \frac{\partial U}{\partial y} + \rho W \frac{\partial U}{\partial z} = \rho g_x - \frac{\partial P}{\partial x} + \frac{\partial}{\partial x} \left[2\eta \frac{\partial U}{\partial x} - \rho u u \right] + \frac{\partial}{\partial y} \left[\eta \left(\frac{\partial U}{\partial y} + \frac{\partial V}{\partial x} \right) - \rho u v \right] + \\ + \frac{\partial}{\partial z} \left[\eta \left(\frac{\partial U}{\partial z} + \frac{\partial W}{\partial x} \right) - \rho u w \right] + S_\omega + S_{DR} \\ \rho \frac{\partial V}{\partial t} + \rho U \frac{\partial V}{\partial x} + \rho V \frac{\partial V}{\partial y} + \rho W \frac{\partial V}{\partial z} = \rho g_y - \frac{\partial P}{\partial y} + \frac{\partial}{\partial y} \left[2\eta \frac{\partial V}{\partial y} - \rho v v \right] + \frac{\partial}{\partial x} \left[\eta \left(\frac{\partial U}{\partial y} + \frac{\partial V}{\partial x} \right) - \rho u v \right] + \\ + \frac{\partial}{\partial z} \left[\eta \left(\frac{\partial V}{\partial z} + \frac{\partial W}{\partial y} \right) - \rho v w \right] + S_\omega + S_{DR} \\ \rho \frac{\partial W}{\partial t} + \rho U \frac{\partial W}{\partial x} + \rho V \frac{\partial W}{\partial y} + \rho W \frac{\partial W}{\partial z} = \rho g_z - \frac{\partial P}{\partial z} + \frac{\partial}{\partial z} \left[2\eta \frac{\partial W}{\partial z} - \rho w w \right] + \frac{\partial}{\partial x} \left[\eta \left(\frac{\partial U}{\partial z} + \frac{\partial W}{\partial x} \right) - \rho u w \right] + \\ + \frac{\partial}{\partial y} \left[\eta \left(\frac{\partial V}{\partial z} + \frac{\partial W}{\partial y} \right) - \rho v w \right] + S_\omega + S_{DR} \end{aligned} \quad (8)$$

energy equation:

$$\begin{aligned} \rho c_p \frac{\partial T}{\partial t} + \rho c_p U \frac{\partial T}{\partial x} + \rho c_p V \frac{\partial T}{\partial y} + \rho c_p W \frac{\partial T}{\partial z} = \frac{\partial}{\partial x} \left[k \frac{\partial T}{\partial x} - \rho c_p u T' \right] + (9) \\ + \frac{\partial}{\partial y} \left[k \frac{\partial T}{\partial y} - \rho c_p v T' \right] + \frac{\partial}{\partial z} \left[k \frac{\partial T}{\partial z} - \rho c_p w T' \right] + q_v \end{aligned}$$

The averaging process has produced extra terms in the momentum and energy equations. For turbulent flow, equations of continuity, of momentum and energy is a system of 5 equations with 14 unknowns [10]. To solve, it is used Boussinesq approximation which defines an eddy viscosity and eddy conductivity:

$$\eta_t = \frac{-\rho u u}{2 \frac{\partial U}{\partial x}} = \frac{-\rho u v}{\frac{\partial U}{\partial y} + \frac{\partial V}{\partial x}} = \frac{-\rho v w}{\frac{\partial V}{\partial z} + \frac{\partial W}{\partial y}} = \dots, \quad (10)$$

$$k_t = \frac{-\rho c_p u t}{\frac{\partial T}{\partial x}} = \frac{-\rho c_p v t}{\frac{\partial T}{\partial y}} = \frac{-\rho c_p w t}{\frac{\partial T}{\partial z}}. \quad (11)$$

These terms imply that the effect of turbulence is isotropic. With these approximations the governing equations become:

$$\frac{\partial \rho}{\partial t} + \frac{\partial \rho u}{\partial x} + \frac{\partial \rho v}{\partial y} + \frac{\partial \rho w}{\partial z} = 0 \quad (12)$$

$$\begin{aligned} \rho \frac{\partial U}{\partial t} + \rho U \frac{\partial U}{\partial x} + \rho V \frac{\partial U}{\partial y} + \rho W \frac{\partial U}{\partial z} &= \rho g_x - \frac{\partial P}{\partial x} + \frac{\partial}{\partial x} \left[2(\eta + \eta_t) \frac{\partial U}{\partial x} \right] + \frac{\partial}{\partial y} \left[(\eta + \eta_t) \left(\frac{\partial U}{\partial y} + \frac{\partial V}{\partial x} \right) \right] \\ &+ \frac{\partial}{\partial z} \left[(\eta + \eta_t) \left(\frac{\partial U}{\partial z} + \frac{\partial W}{\partial x} \right) \right] + S_w + S_{DR} \\ \rho \frac{\partial V}{\partial t} + \rho U \frac{\partial V}{\partial x} + \rho V \frac{\partial V}{\partial y} + \rho W \frac{\partial V}{\partial z} &= \rho g_y - \frac{\partial P}{\partial y} + \frac{\partial}{\partial y} \left[2(\eta + \eta_t) \frac{\partial V}{\partial y} \right] + \frac{\partial}{\partial x} \left[(\eta + \eta_t) \left(\frac{\partial U}{\partial y} + \frac{\partial V}{\partial x} \right) \right] \\ &+ \frac{\partial}{\partial z} \left[(\eta + \eta_t) \left(\frac{\partial V}{\partial z} + \frac{\partial W}{\partial y} \right) \right] + S_w + S_{DR} \\ \rho \frac{\partial W}{\partial t} + \rho U \frac{\partial W}{\partial x} + \rho V \frac{\partial W}{\partial y} + \rho W \frac{\partial W}{\partial z} &= \rho g_z - \frac{\partial P}{\partial z} + \frac{\partial}{\partial z} \left[2(\eta + \eta_t) \frac{\partial W}{\partial z} \right] + \frac{\partial}{\partial x} \left[(\eta + \eta_t) \left(\frac{\partial U}{\partial z} + \frac{\partial W}{\partial x} \right) \right] \\ &+ \frac{\partial}{\partial y} \left[(\eta + \eta_t) \left(\frac{\partial V}{\partial z} + \frac{\partial W}{\partial y} \right) \right] + S_w + S_{DR} \end{aligned} \quad (13)$$

$$\begin{aligned} \rho c_p \frac{\partial T}{\partial t} + \rho c_p U \frac{\partial T}{\partial x} + \rho c_p V \frac{\partial T}{\partial y} + \rho c_p W \frac{\partial T}{\partial z} &= \frac{\partial}{\partial x} \left[(k + k_t) \frac{\partial T}{\partial x} \right] \\ &+ \frac{\partial}{\partial y} \left[(k + k_t) \frac{\partial T}{\partial y} \right] + \frac{\partial}{\partial z} \left[(k + k_t) \frac{\partial T}{\partial z} \right] + q_v \end{aligned} \quad (14)$$

In these conditions should be determined in addition to the 5 unknowns only k_t and η_t . The program COSMOS Flow uses a model with two equations for their determination [10]:

$$\eta_t = \frac{C_\eta \rho K^2}{\varepsilon}, \quad (15)$$

$$k_t = \frac{\eta_t c_p}{Pr_t}, \quad (16)$$

where Pr_t - turbulent Prandtl number and C_η - empirical constant. The transport equations for K and ε are derived using momentum equations:

$$\begin{aligned} \rho \frac{\partial K}{\partial t} + \rho U \frac{\partial K}{\partial x} + \rho V \frac{\partial K}{\partial y} + \rho W \frac{\partial K}{\partial z} &= \frac{\partial}{\partial x} \left[\left(\frac{\eta_t}{\sigma_k} + \eta \right) \frac{\partial K}{\partial x} \right] + \frac{\partial}{\partial y} \left[\left(\eta + \frac{\eta_t}{\sigma_k} \right) \left(\frac{\partial K}{\partial y} \right) \right] \\ &+ \frac{\partial}{\partial z} \left[\left(\eta + \frac{\eta_t}{\sigma_k} \right) \left(\frac{\partial K}{\partial z} \right) \right] - \rho \varepsilon + \eta_t \left[2 \left(\frac{\partial U}{\partial x} \right)^2 + 2 \left(\frac{\partial V}{\partial y} \right)^2 + 2 \left(\frac{\partial W}{\partial z} \right)^2 + \left(\frac{\partial U}{\partial y} + \frac{\partial V}{\partial x} \right)^2 + \left(\frac{\partial U}{\partial z} + \frac{\partial W}{\partial x} \right)^2 + \left(\frac{\partial V}{\partial z} + \frac{\partial W}{\partial y} \right)^2 \right] \end{aligned} \quad (17)$$

$$\begin{aligned} \rho \frac{\partial \varepsilon}{\partial t} + \rho U \frac{\partial \varepsilon}{\partial x} + \rho V \frac{\partial \varepsilon}{\partial y} + \rho W \frac{\partial \varepsilon}{\partial z} &= \frac{\partial}{\partial x} \left[\left(\frac{\eta_t}{\sigma_\varepsilon} + \eta \right) \frac{\partial \varepsilon}{\partial x} \right] + \frac{\partial}{\partial y} \left[\left(\eta + \frac{\eta_t}{\sigma_\varepsilon} \right) \left(\frac{\partial \varepsilon}{\partial y} \right) \right] \\ &+ \frac{\partial}{\partial z} \left[\left(\eta + \frac{\eta_t}{\sigma_\varepsilon} \right) \left(\frac{\partial \varepsilon}{\partial z} \right) \right] - \rho C_2 \frac{\varepsilon^2}{K} + C_1 \eta_t \frac{\varepsilon}{K} \left[2 \left(\frac{\partial U}{\partial x} \right)^2 + 2 \left(\frac{\partial V}{\partial y} \right)^2 + 2 \left(\frac{\partial W}{\partial z} \right)^2 + \left(\frac{\partial U}{\partial y} + \frac{\partial V}{\partial x} \right)^2 + \left(\frac{\partial U}{\partial z} + \frac{\partial W}{\partial x} \right)^2 + \left(\frac{\partial V}{\partial z} + \frac{\partial W}{\partial y} \right)^2 \right] \end{aligned} \quad (18)$$

where σ_K and σ_ε - turbulent Schmidt numbers, C_1 , C_2 - empirical constants. With these 2 equations, there are 9 equations in 9 unknowns: $U, V, W, P, T, \mu_t, k_t, K, \varepsilon$. Table 3 presents the constants associated to model [10].

Constant	Value
C_η	0.09
C_1	1.44
C_2	1.92
σ_k	1.0
σ_ε	1.3

Table 3. Constants used in model

4 The realized analysis, using finite element analysis

Researchers found a lot of ways to solve the equations in fluid flow domain. A reliable numerical technique often used is finite element method (FEM). This is used to discretize the flow domain, thereby transforming the governing partial differential equations into a set of algebraic equations whose solution represents an approximation to the exact analytical solution [9].

In this paper Cosmos/Flow program is used for solving heat and momentum transfer equations in a moving fluid [10]. It is applied the Streamline Upwind Petrov Galerkin (SUPG) method [10]. The method is used directly on the diffusion and source terms and for the advection terms, the streamline upwind method is used with the weighted integral method. These terms are transformed to stream-wise coordinates, like in next expression[10]:

$$\rho U \frac{\partial \phi}{\partial x} + \rho V \frac{\partial \phi}{\partial y} + \rho W \frac{\partial \phi}{\partial z} = \rho U_s \frac{\partial \phi}{\partial S}, \quad (19)$$

where s – stream-wise coordinate, U_s – the velocity component in the stream-wise coordinate direction, Φ -transported quantity.

In figure 4 is shown the used analysis scheme. A set of simplified hypothesis are introduced for realize the mathematical models:

- Hot water and cold water are Newtonian fluids;
- No phase change occurs, the fluids are unmixed;
- Turbulent flow is fully developed;
- Working fluids are incompressible,
- Steady state conditions;
- Coefficient of heat retention equal with 1.

In COSMOS/Flow it is open the 3D model and it is defined the case study, by specifying the name, analysis type, the disparagement mode. The study is fluid flow type and the analysis is thermal (result type: permanent or transient, the iterative resolving technique: Newton-Raphson scheme, initial temperature and calculus tolerance) [9].

After those, it applied mesh, the disparagement mode, which is very important for the final results. The models are divided in a multitude of little parts with simple geometrical forms, defined as finite parts, and connected in common points called nodes. From analysis point of view, FEM accounts the different behavior of each part depending of the imposed conditions, the global behavior of the model being calculated from the totality of calculated information for all the finite elements of the model [10].

The mesh quality depends on the active mesh options. In this case, the quality of mesh is high (10-node tetrahedral). Mesh type is solid mesh. The number of elements and nodes associated with the studied geometry are given in table 4.

For incompressible flows, the most robust condition for the pressure equation is to specify a value at the outlet. Since only relative pressures are calculated by COSMOS/Flow, a value of 0 is recommended [10].

Number of plates	Nodes	Elements	Element size [mm]
3	110610	72159	5,2306
4	147265	99046	5,3894
5	169261	115136	5,8804
6	186844	127891	6,6008
7	218811	151027	6,6714
8	238019	164897	7,005
9	259729	180407	7,3094
10	286491	199604	7,5904

Table 4. Detail of mesh

The numerical simulation of turbulent flow is modeled by k - ϵ turbulence model. ϵ represents the turbulent

energy dissipation. To calculate the boundary layer, either “wall functions” are used, overriding the calculation of k and ϵ in the wall adjacent nodes, or integration is performed to the surface, using a “low turbulent Reynolds ($low-Re$) k - ϵ ” model [5],[11].

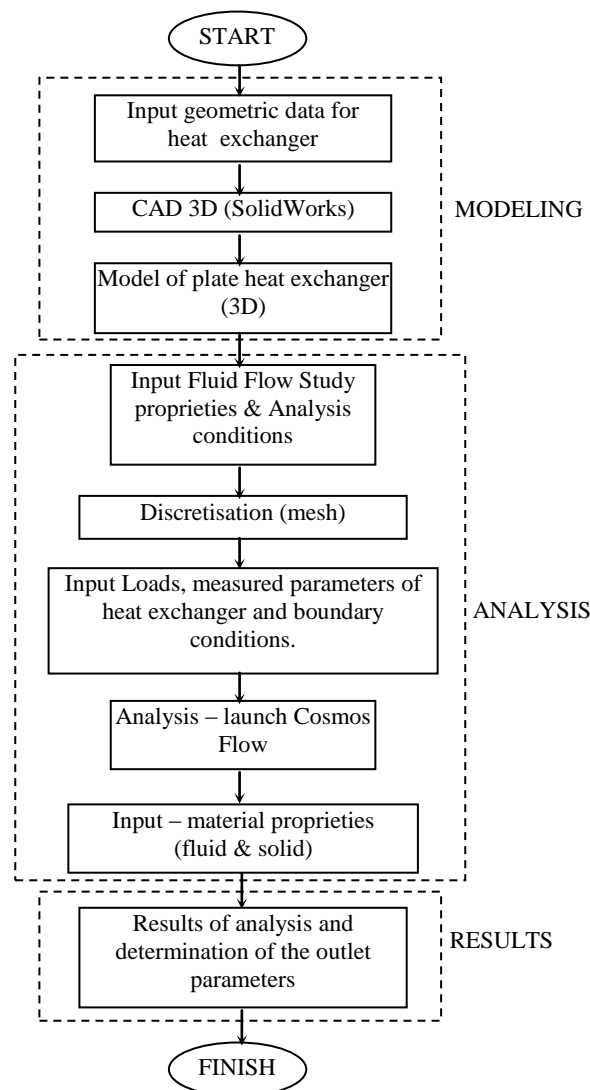


Fig.4. Analysis scheme

For all eight cases are proposed the next boundary conditions:

No.	Fluid	Description	Unit	Value
1	Hot Water inlet	Temperature $T_{1,in}$	°C	53
2		Velocity, v_1	m/s	0,303
4	Cold Water inlet	Temperature $T_{2,in}$	°C	8
5		Velocity, v_2	m/s	0,26

6	Hot water outlet	Static pressure	N/m^2	0
7	Cold water outlet	Static pressure	N/m^2	0
8	Air	Convection on exterior plate, α	W/m^2K	5
9	Air	Convection on exterior plate, α	W/m^2K	5

Table 5. Inlet data for analysis

In figure 5 is shown the disparagement mode for the model of heat exchanger with 7 plates. It is very important to realize the mesh with great accurately. In the case of high quality mesh, time for analyze running is very big.

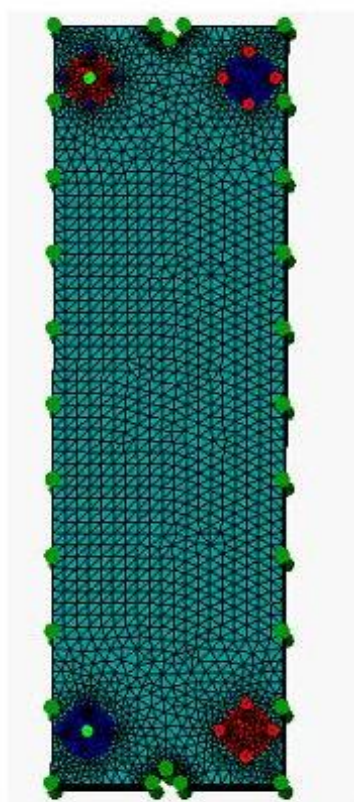


Fig.5. Mesh

5 Results

After the analysis was processed it can be visualized the results, under graphical form or numerical value. Because the governing equations are non-linear, they must be solved iteratively. A Picard or successive

substitution is used [10]. In this method estimates of the solution variables are substituted in the governing equations. The equations are solved for new values which are the used as the estimates for the next pass. The convergence criterion is the level at which the specified variable's residual norm must reach. With each pass, the residuals should become smaller if the solution is converging. The global iterations is shown below:

1. Solve x momentum equation
2. Solve y momentum equation
3. Solve z momentum equation
4. Solve pressure equation and velocities
5. Solve energy equation
6. Solve turbulent kinetic energy equation
7. Solve turbulent energy dissipation equation
8. Check convergence (GOTO1)

Analysis runs for 100 iterations, in turbulence conditions, for all eight cases. Profiles are obtained for the following parameters: u , v , w , T , k , ε .

In figure 6 is presented the distribution of the nodal temperature, after 100 iterations, for the heat exchanger with eight plates.

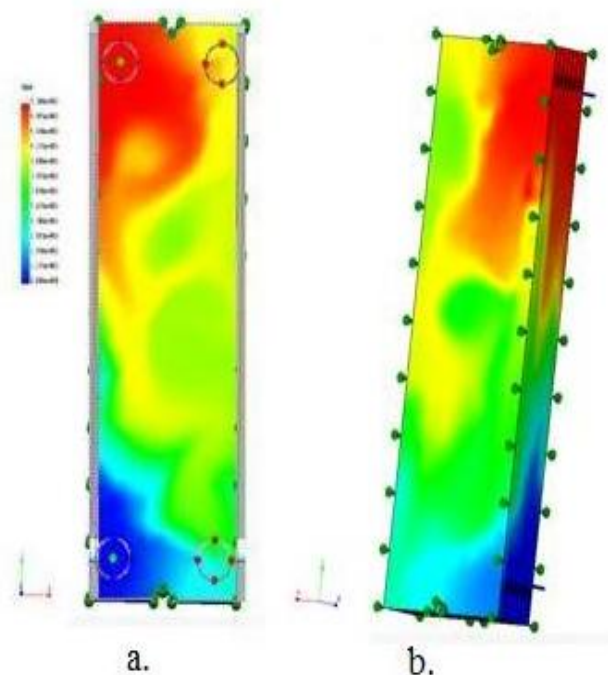


Fig.6. Distribution of the temperature: a. front view, b. rear view, 8 plates

Figure 7 show the distribution of the temperature on the side view for the counter flow heat exchanger with three plates, after 100 iterations.

Convergence control of a solution variable is accomplished by reduction the solution progression rate so that the change of divergence is minimized. COSMOS/Flow has the Graphical Convergence Monitor, where are presented the numerical data like the

average, the average, minimum, maximum values for each degree of freedom over the completed range of iterations.

the solution can be considered converged after 100 iterations. This is true for all eight cases studied.

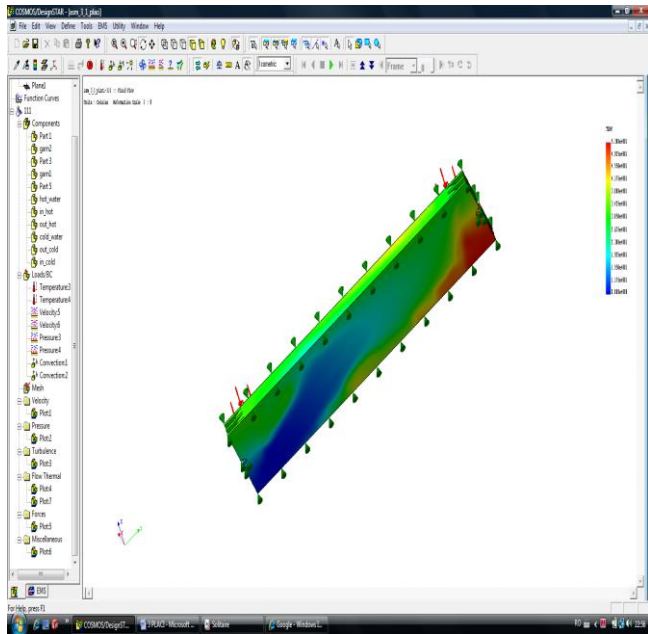


Fig.7. Distribution of the temperature, side view, 3 plates

In figure 8 is shown the convergence for the average value of the temperature in case of heat exchanger with seven plates.

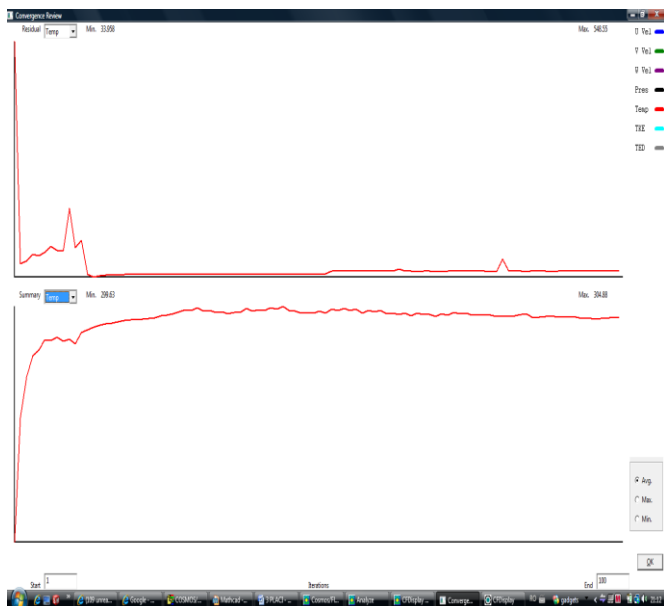


Fig.8. Convergence for average value of temperature, heta exchanger with 7 plates

On the computer monitor can view results as shown in figure 9. It is observed that all the resulted parameters asymptotes to a single value. This is important because

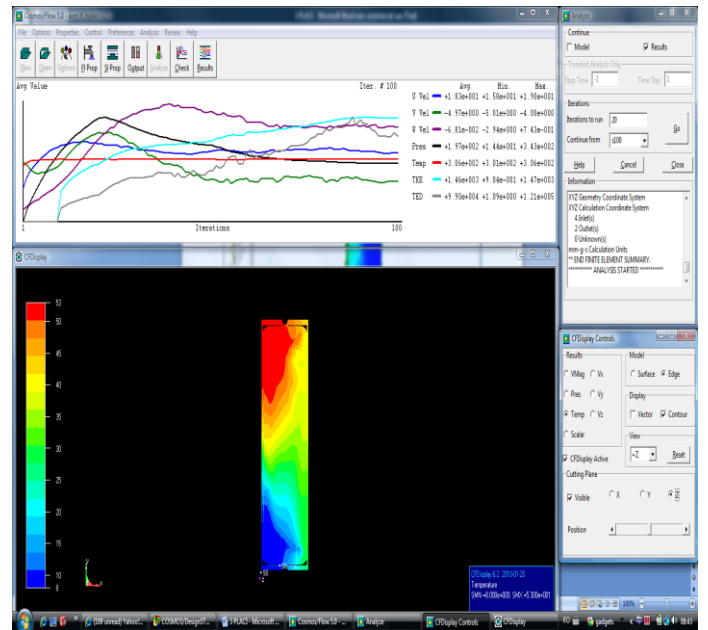


Fig.9. Results displayed on the monitor

The values obtained for average temperature at the outlet of hot water and outlet of cold water are presented in table 6.

Number of plates N_p	Hot water outlet $T_{1,out}$ [°C]	Cold water outlet $T_{2,out}$ [°C]
	3	31,8
4	25,2	40,2
5	27,8	37,4
6	22,7	43,2
7	23,4	42,4
8	22	44,1
9	22,08	43,9
10	21,4	44,7

Table 6. Determined values of average temperatures

As expected, it is observed that with increasing number of plates, cold water temperature at outlet, increase, too. Faster growth is obtained for heat exchangers with even number plates. In these cases, there is an extra hot-water channel, under the original construction considerations.

Knowing for both agents, flow volumes, $V_1' = 1,905 \cdot 10^{-4} \text{ m}^3/\text{s}$ for hot water and $V_2' = 1,633 \cdot 10^{-4} \text{ m}^3/\text{s}$ for cold water and knowing thermodynamic proprieties, we can determine flow stream heat capacity rates for all cases.

Formulas for heat capacity rates are:

$$C_1 = V'_1 \times c_{p,1} \times \rho_1 \cdot [\text{W/K}] \quad (20)$$

$$C_2 = V'_2 \times c_{p,2} \times \rho_2 \cdot [\text{W/K}] \quad (21)$$

$$LMTD = \frac{\Delta T_{max} - \Delta T_{min}}{\ln\left(\frac{\Delta T_{max}}{\Delta T_{min}}\right)} \quad (23)$$

where c_p [J/kgK] – heat capacity at constant pressure, ρ [kg/m³] – density.

Minimum heat capacity rate is:

$$C_{min} = \min(C_1, C_2) \cdot [\text{W/K}] \quad (22)$$

where $\Delta T_{max} = \max(\Delta T_1, \Delta T_2)$, $\Delta T_{min} = \min(\Delta T_1, \Delta T_2)$; $\Delta T_1, \Delta T_2$ from figure 9.

Heat exchanger effectiveness ϵ is determined with relation (23).

$$\epsilon = \frac{C_1 \times (T_{1,in} - T_{1,out})}{C_{min} \times (T_{1,in} - T_{2,in})} = \frac{C_2 \times (T_{2,out} - T_{2,in})}{C_{min} \times (T_{1,in} - T_{2,in})} \quad (24)$$

We study separately heat exchangers with even number of plates and heat exchangers with odd number of plates, and after that, we compare the results.

Number of plates N_p	Hot water outlet	Cold water outlet	C_{min} [W/K]
	C_1 [W/K]	C_2 [W/K]	
3	789,198	681,828	681,828
4	790,152	680,883	680,883
5	789,778	681,227	681,227
6	790,509	680,519	680,519
7	790,408	680,616	680,616
8	790,608	680,410	680,410
9	790,597	680,435	680,435
10	790,693	680,338	680,338

Table 7. Heat capacity rates

N_p	3	5	7	9
$LMTD$	22,056	17,616	12,851	11,409
ϵ	0,547	0,653	0,764	0,798

Table 8. Results for heat exchanger with an odd number of plates

We observe that $C_1 > C_2$.
The hot and cold water temperature distributions in the counter-flow heat exchanger are shown in figure 10.

N_p	4	6	8	10
$LMTD$	14,892	12,085	11,258	10,647
E	0,716	0,782	0,802	0,816

Table 9. Results for heat exchanger with an even number of plates

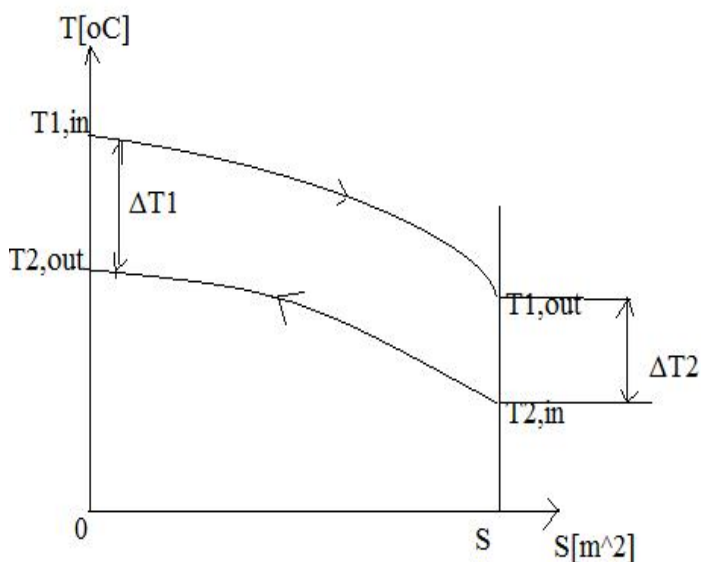


Fig. 10. The hot and cold fluid temperature distributions in the counter flow heat exchanger

$LMTD$ – log mean temperature difference is computed under assumption of counter flow condition with next relation [1]:

In these cases, the efficiency of exchangers with an even number of plates is greater than that of those with odd number plates. One explanation is that exchangers with an even number of plates has the number of flow channels for hot water is one greater than for cold water. The efficiency changes depending on the number of plates are shown in figure 11.

It is noted that even versus odd number of plates have a strong influence for $N_p < 8$ and for $N_p = 9, N_p = 10$ a negligible influence (the increase in ϵ is insignificant). The same applies to cold water temperature at outlet. The paper [4] presented similar findings, extended for $N_p = 40$ plates.

In figure 12 are shown the variations of cold water temperature at the outlet depending on the number of plates. There is a higher growth for exchanger with even number of plates. The variation of $LMTD$ depending on the number of plates is presented in figure 13.

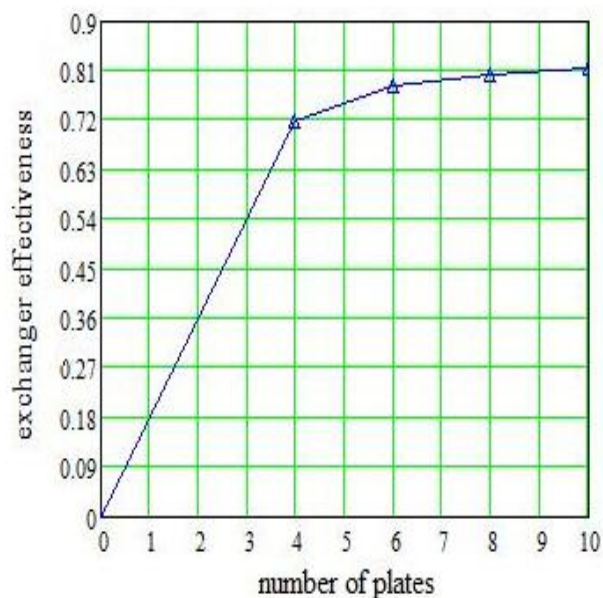
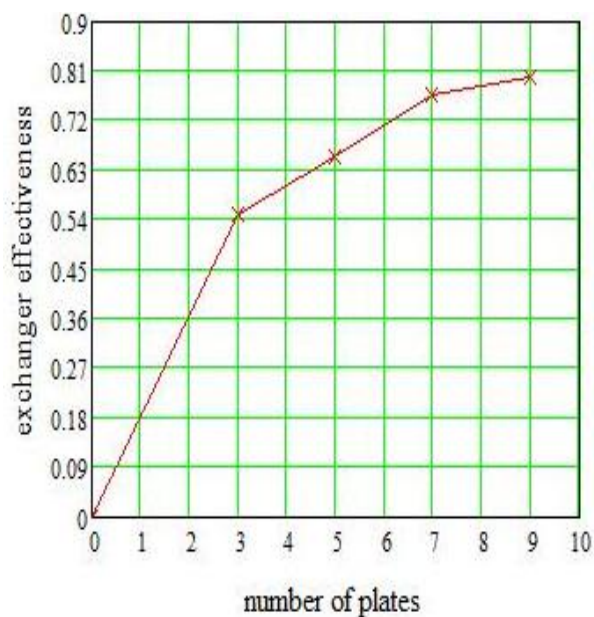


Fig. 11. The influences of the number of plates for 1pass-1 pass counter-flow heat exchanger effectiveness: a. odd number of plates, b. even number of plates

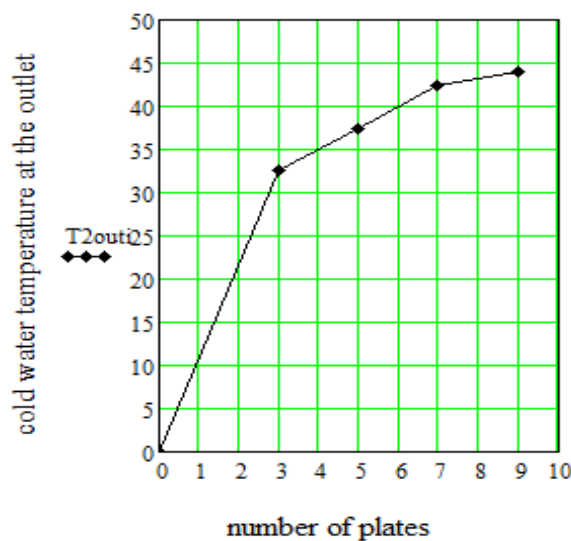
6 Conclusions

The conducted research about the counter-flow plate heat exchanger, using finite element method, represents an important tool for study the fluid flow distribution and heat transfer in a plate heat exchanger. In the sometime, the model is perfectible and offers good information about the behavior of counter-flow plate heat exchanger in different conditions of

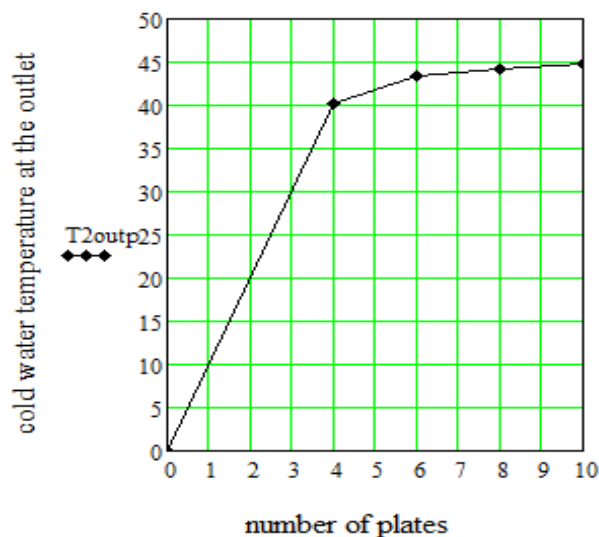
operation and it can be integrated in a more complex system [9],[12].

Numerical results are presented for 1 pass-1 pass counter-flow heat exchangers. These results are shown in terms of cold water temperature at the outlet, hot water temperature at the outlet, exchanger effectiveness and log –mean temperature difference as functions of the heat capacity ratio and the number of plates.

As future work will be accomplished the study of heat exchanger with even number of plates for which the number of flow channels for cold water is one greater than for hot water.



a.



b.

Fig. 12. The influences of the number of plates for 1pass-1 pass counter-flow heat exchanger cold water temperature at the outlet: a. odd number of plates, b. even number of plates

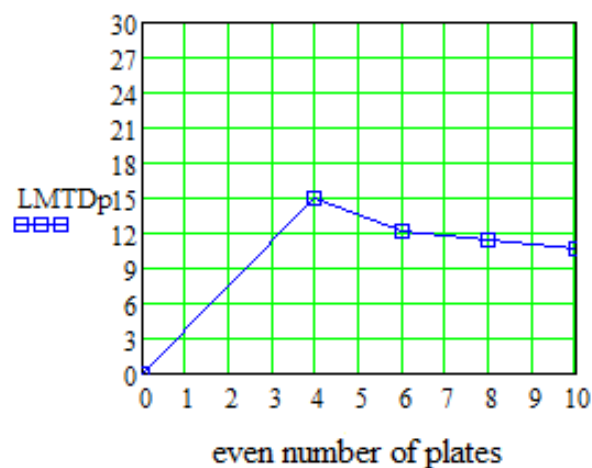


Fig. 13. The influences of the number of plates for 1pass-1 pass counter-flow heat exchanger LMTD

References:

- [1] A. Badea, H. Necula, M. Stan, L. Ionescu, P. Blaga., G.Darie, *Echipamente și instalații termice*, Editura Tehnică, București, 2003
- [2] J. A. W. Gut, J. M. Pinto, *Modeling of plate heat exchangers with generalized configurations*, International Journal of Heat and Mass Transfer, 2003, pp. 2571-2585.

- [3] Z. Zhang, Y. Zhong Li, *CFD simulation on inlet configuration of plate-fin heat exchangers*, Cryogenics 43 (2003) pp. 673–678, www.elsevier.com/locate/cryogenics.
- [4] L.Garba, S.Mehes, *Heat Capacity of Vertical Ground Heat Exchangers with Single U-Tube Installation in the Function of Time*, WSEAS Transactions on Heat and Mass Transfer, vol. 3, 2008, pp. 177-186
- [5] D.Cotoros, M.Baritz, L.Cristea, *Assessment of Heat Exchangers Based on the Efficiency Coefficient*, 6th IASME/WSEAS International Conference on HEAT TRANSFER, THERMAL ENGINEERING and ENVIRONMENT, Rhodes, Greece, August 20-22 2008, pp.318-321
- [6] R.K.Shah, S.G.Kandlikar, *The Influence of the Number of Thermal Plates on Plate Heat Exchanger Performance*, www.rit.edu
- [7] A.G.Kanaris, K.A.Mouza, S.P.Paras, *Designing Novel Compact Heat Exchangers for Improved Efficiency using a CFD Code*, 1st International Conference „From Scientific Computing to Computational Engineering”, Athens, Greece, 2004
- [8] R.Grigore, S.Popa, *Some Aspects about Numerical Simulation of Plate Heat Exchanger Using Finite Element Method*, 7th International Conference on Electromechanical and Power Systems SIELMEN 2009, Iași, Romania
- [9] R.Grigore, S.Popa, *Modeling a Counter-flow Plate Heat Exchanger*, 4TH International Conference on Energy and Environment, CIEM 2009,–București, Romania
- [10] *** COSMOS/Flow - Technical Reference
- [11] M.H.Saber, H.Mazaher Ashtiani, *Simulation and CFD Analysis of heat pipe exchanger using Fluent to increase of the thermal efficiency*, 5th IASME/WSEAS International Conference on Continuum Mechanics, University of Cambridge, UK, February 23-25, 2010, pp.184-189
- [12] F.D.Surianu, C.Barbulescu, *Complete Dynamic Behaviour Mathematical Modelling of Hydromechanical Equipment. Case Study: Hydro Power Plant Raul Mare – Retezat, Romania*, WSEAS Transactions on Power Systems, Issue 7, vol.3, 2008, pp. 517-526